Asian Journal of Water, Environment and Pollution. Vol. 22, No. 3 (2025), pp. 134-152.
doi: 10.36922/AJWEP025150107

ORIGINAL RESEARCH ARTICLE

Projected trends in extreme heat in Senegal from 2020 to 2080

Moussa Sow[1] and Demba Gaye[2]*

[1]Department of Environment, Biodiversity and Sustainable Development, Faculty of Social and Environmental Sciences, Sine Saloum El-Hadj Ibrahima Niass University, Kaolack, Senegal
[2]Laboratory of Geomatics and Environment, Department of Geography, Faculty of Sciences and Technology, Assane Seck University, Ziguinchor, Senegal
***Corresponding author:** Demba Gaye (demba.gaye@univ-zig.sn)

Received: April 08, 2025; 1st revised: May 03, 2025; 2nd revised: May 12, 2025; Accepted: May 14, 2025; Published Online: June 10, 2025

Abstract: Faced with the challenges that climate change poses to all human societies, adaptation is becoming a necessity for human survival. In this context, it is necessary to study the climatic phenomena that humans face and that are likely to impact various aspects of life. Therefore, this study sought to analyze the trend of heat waves in Senegal using data from the Coupled Model Intercomparison Project Phase 6 (CMIP6), Canadian Earth System Model Version 5. Three climate scenarios (Shared Socioeconomic Pathway [SSP]1-2.6, SSP2-4.5, and SSP5-8.5) were used, and the study focused on two future climate normals (2020 – 2050, 2050 – 2080). The study first spatialized the 95th percentile of minimum, mean, and maximum temperatures, then analyzed temperature anomalies with the Lamb index before studying the future trend using the Mann-Kendall test. The results obtained reflect an upward trend for all the variables in this study for the two periods combined but with a different level of significance. This increase is greater for minimum temperatures, with rises of 0.43°C for SS1-2.6, 1.06°C for SSP2-4.5, and 2.18°C for SSP5-8.5. In comparison, maximum temperatures rose by 0.50°C, 1.05°C, and 2.03°C, respectively, between the first and second periods. Mean temperatures followed the same dynamic, with 0.48°C for SSP1-2.6, 1.04°C for SSP2-4.5, and 2.16°C for SSP5-8.5. Given these findings, it is important to analyze the behavior of the other CMIP6 models in assessing heat waves in Senegal.

Keywords: Future trends; Heat waves; Mann–Kendall test; Canadian Earth System Model Version 5; Coupled Model Intercomparison Project Phase 6; Senegal

1. Introduction

Climate change is considered one of the greatest risks of the 21st century, with the potential to affect the health and lives of billions of people worldwide.[1] This phenomenon is defined as the consequence of the intensification of anthropogenic greenhouse gas emissions.[2,3] It is also a factor influencing public health, with diverse and potentially catastrophic consequences.[4] In this context, studies have shown that the global average temperatures are expected to increase by 5.5°C by the end of the 21st century,[5] which might result in a global intensification, recurrence, and sustainability of heat waves.[6,7] The increased exposure to heat waves is expected to deteriorate population health, increasing heat-related mortality and morbidity globally.[8]

In addition, climate forecasts for the 21st century suggest a greater increase in temperatures in Africa

compared to the global average, with an intensification of extreme heat events.[9] Therefore, the frequency, duration, and severity of heat waves are expected to intensify in the future.[2,10] The projected effects of heat waves are expected to impact both social and economic sectors. First, heat waves are expected to pose a significant risk to human health.[11] The adverse effects on health will be more noticeable in impoverished regions, where limited health coverage hinders adaptation and proper care.[12] In fisheries, these extreme heat events result in the degradation of marine habitats, and negatively impact the conditions required for the survival of local biodiversity.[13] In terms of agriculture, prolonged heat compromises photosynthesis activity and promotes the proliferation of pests, both of which lead to a decline in agricultural yields.[14,15]

Understanding this phenomenon is essential for adapting to its impacts. However, studies on hot extremes in Africa have only been conducted recently, unlike in Europe and America, where heat waves have been extensively documented. This scarcity of studies is concerning given the increasing temperatures in Africa and the insufficient adaptation measures, which are closely linked to the lack of climate data in the region.[16]

Particularly in the Sahelian region of Africa, there are significant challenges in access and availability of climate data. On one hand, access is hindered by exorbitant costs in many countries.[17] On the other hand, following the structural adjustment policies of the 90s, the observation network has been underdeveloped, leading to incomplete or even data shortage over time.[18] This partly explains the scarcity of studies on hot extremes in Africa, particularly in the Sahelian region. In addition, the continent is facing other pressing priorities, such as flooding, whose impacts are more noticeable than hot extremes.

The challenge of limited data has been mitigated by climate modeling, which is capable of tracing past and present climate changes, as well as predicting future ones. Climate models have become much more complex to better represent physical and environmental processes at increasingly fine scales.[19] Therefore, numerous studies have focused on the prospective evolution of the climate. Heat waves and their health impacts highlight the importance of climate models for strategizing mitigation and adaptation efforts.[20] The advent of climate data now makes it possible to predict future temperature trends with greater regional and even local detail, especially with the contribution of regionalized climate models.

The present study aimed to analyze the future trend of heat waves in Senegal over the periods of 2021 – 2050 and 2051 – 2080 according to the Coupled Model Intercomparison Project Phase 6 (CMIP6) scenarios of Shared Socioeconomic Pathway (SSP)1-2.6, SSP2-4.5, and SSP5-8.5. The main objectives of this study were to: (i) spatialize the 95th percentile of mean, minimum, and maximum temperatures; (ii) study anomalies; and (iii) analyze the trend of heat waves over the periods 2021 – 2050 and 2051 – 2080. The studies focusing on heat waves in Senegal using CMIP6 are limited. This is the first study applying the CMIP6 Canadian Earth System Model Version 5 (CanESM5) model to project Senegal's extreme heat trends. Therefore, this study extends several previous researches performed by Toure *et al*.,[21] Sow *et al*.,[22] Sow *et al*.,[23] Sow and Gaye,[24] and Sy *et al*.,[25] which tried to address the health impacts of heat waves in the northeastern regions of Senegal.

2. Materials and methods

2.1. Study area

Senegal is a country located on the West Coast of Africa. It is distinguished by its coastline stretching about 700 km. Senegal extends between latitudes 12°5 and 16°5 North and longitudes 11°5 and 17°5 West (Figure 1). Bordering Mauritania to the north, Mali to the east, the republics of Guinea and Guinea-Bissau to the south, and the Atlantic Ocean to the west, it is a country with a relatively homogeneous terrain with altitudes rarely exceeding 50 m.[26,27] Some massifs remain mainly in the eastern part of the country, such as the Fouta Djalon, which rises to 581 m, but the altitude decreases toward the west to 15 m toward the mouth of the Senegal River. The generally low terrain favors an unconstrained atmospheric circulation, subjecting the territory to a Sudano-Sahelian-type climate dominated by maritime trade winds, continental trade winds (commonly known as the Harmattan), and monsoon air masses. Under the influence of these defined air masses, two distinct seasons emerge each year: a long dry season and a rainy season. Soil science, on the other hand, is characterized by soils that are very vulnerable to degradation, particularly water and wind erosion. The hydrological potential is significant due to the presence of several rivers and lakes, such as the Senegal River, the Gambia River, the Casamance River, the Geba River, and the Lake of Guiers, which provide substantial water resources. However, the country's water availability is highly dependent on the amount and distribution of rainfall.[28] Annual rainfall totals range from <300 mm in the north to more than 1000 mm in the southern part of Senegal.[29] The temperature ranges from 16°C to

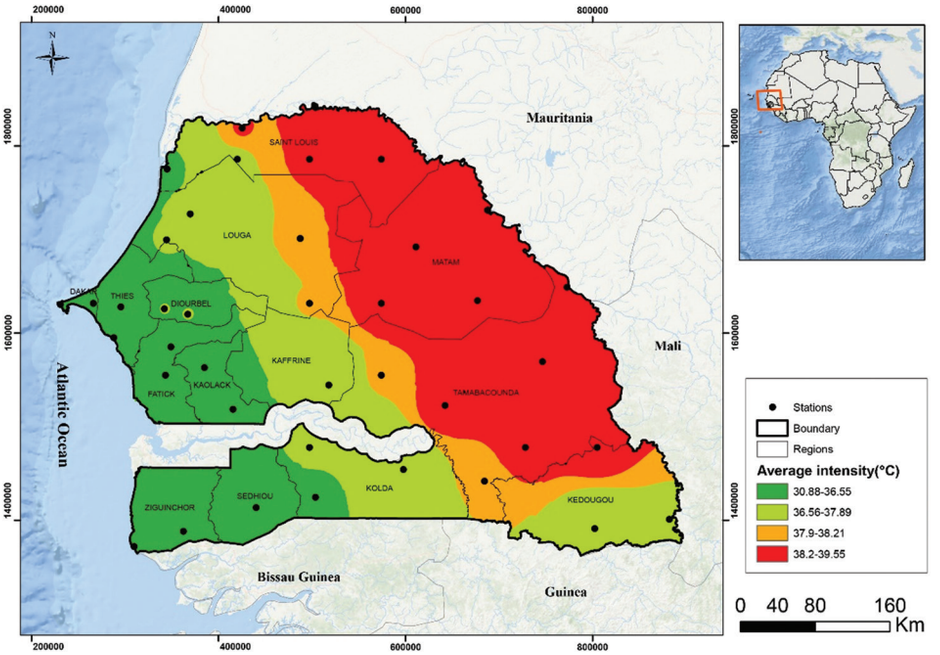

Figure 1. Distribution of heat wave intensity across Senegal from 1984 to 2020. Figure created with ArcGis 10.8, Sow and Gaye (2025).

30°C along the coastal strip, under the influence of the Atlantic Ocean, and can reach up to 40°C in the central and eastern regions of the country, which are subjected to the effects of continentality.[30]

2.2. Materials

To analyze the future trend of heat waves, CMIP6 simulation data were collected. Compared to the Coupled Model Intercomparison Project Phase 5 (CMIP5), CMIP6 introduces several improvements in physical modeling and resolution. CMIP6 is the result of two decades of research on the comparison of climate models.[19] It is an update of CMIP5 that incorporates socio-economic parameters.[31] Several studies have used CMIP6 data across various fields.[32-34] Some authors have concluded that CMIP6 performs better than CMIP5 models.[35,36] For instance, Mmame and Ngongondo[32] report that CMIP6 models provide substantial improvements in the simulation of temperature and precipitation, with biases often below 10%. In this study, the CanESM5 model was used as input. This model was developed by the Canadian Center for Climate Modelling and Analysis and is available on the World Climate Research Programme (WCRP). It is an improved version of the Second Generation Canadian Earth System Model.[37] Atmospheric blocking, which is often the cause of heat waves,[38] was observed with this model by Arora *et al.*[39] and Brunner *et al.*[40] over the historical period 1981 – 2010. The CanESM5, with a spatial resolution of 2.8° × 2.8°, enables the illustration of the connections between heat waves and atmospheric blocking.[41] Three scenarios were selected (SSP1-2.6, SSP2-4.5, and SSP6-8.5) for two climatic periods (2021 – 2050 and 2051 – 2080).

The choice of the CanESM5 model was based on a literature review, which highlighted its strong performance in the study of climatic extremes, particularly due to its ability to represent the phenomena responsible for heat waves. Its evolution from version 2 to version 5 has enhanced its simulation capabilities, and its spatial resolution of 2.8° × 2.8° is particularly well-suited to countries, such as Senegal, where climatic conditions vary significantly across regions. The choice of using a single model has been adopted by Brunner *et al.*,[40] Jeong *et al.*,[37] and Schaller *et al.*,[41] allowing us to focus on the specific features and results provided by these models, which are generally validated and adjusted to meet the objectives of each study.

2.3. Methods

2.3.1. Evaluation of the performance of the Canadian Earth System Model Version 5

In the context of using climate model outputs, it is often recommended to conduct evaluations using various methods, including the Kling-Gupta Efficiency (KGE) and Percent Bias (pBias). Various authors, including

Dehban *et al*.,[42] Mmame and Ngongondo,[32] and Zareian *et al*.,[43] have utilized these methods to evaluate the models' ability in reproducing reference data. KGE is a performance metric that indicates the model's ability to reproduce an observed or reference time series. It is calculated based on the correlation coefficient (r), biases (β), and variability (γ) using the following formula:

$$KGE = 1 - \sqrt{(r-1)^2 + (\beta-1)^2 + (\gamma-1)^2} \quad \text{(I)}$$

$$With.\ \beta = \frac{\mu_{sim}}{\mu_{obs}},\ \gamma = \frac{\sigma_{sim}}{\sigma_{obs}}$$

Where:
σ = standard deviation
μ = mean
sim = simulation data
obs = observation data

Percentage Bias is used to evaluate model performance by comparing simulated data to reference or observed data. It accounts for systematic bias in simulated data and indicates the extent to which the model overestimates or underestimates the observed data. The closer the pBias value is to zero, the more accurately the model reproduces the reference data. It is calculated using the following formula:

$$pBiais = \sum_{i=1}^{n} \frac{\left(Qsim[i] - Qobs[i]\right)}{\sum_{i=1}^{n} Qobs(i)} \times 100 \quad \text{(II)}$$

where:
Q = values at time step
n = number of time step

2.3.2. Data resampling and extraction

Canadian Earth System Model Version 5 data have been uploaded to the WCRP platform (https://esgf-node.llnl.gov/search/cmip6/) in netCDF format. They were then resampled to reduce the size of the grids. This operation reduced the data to a spatial resolution of 0.0625° × 0.0625° per grid. The data were then extracted based on the coordinates of the 40 grid points selected for this study (Figure 1), and the 95th annual percentiles of the SSP1-2.6, SSP2-4.5, and SSP6-8.5 scenarios were calculated. In previous studies, Da Silva *et al*.[44] and Teegavarapu *et al*.[45] demonstrated the effectiveness of this approach in capturing the spatial variability of climatic variables in the study area using simulated data. Among the available interpolation methods, we utilized bilinear interpolation,[46,47] implemented through the Climate Data Operator software. This resampling approach has been employed by several authors, including Goudiaby *et al*.[48] and Bodian *et al*.[49] In this study, the 95th percentile was selected as the threshold for detecting heat waves.

2.3.3. Spatialization of extreme heat

The inverse distance weighted (IDW) interpolation method was used to spatialize the results at the scale of Senegal. This is a robust method that allows the estimation of values across a surface based on known data points. It is based on the principle that each measuring point influences its surrounding area, with the influence decreasing as distance increases. This method was used to map the 95th percentile across Senegal.

2.3.4. Heat wave anomalies

The Lamb index (1982) was applied to identify interannual anomalies of extreme heat in Senegal for the periods 2021 – 2050 and 2051 – 2080. This index helps assess the interannual variability of extreme temperatures and detect fluctuations in hydro-climatic regimes[50] and climatic phenomena.[28,51] A positive index indicates an increase in temperatures, while a negative index reflects a decrease.[30]

$$IL = \frac{x_i - x_m}{\sigma} \quad \text{(III)}$$

where:
IL = Lamb index
x_i = 95th annual percentiles for a station during a year
x_m = annual average of the 95th percentile of the mean temperature at the station during the study period.

The trend of extreme heat was obtained using the Mann-Kendall test,[52,53] a non-parametric test that identifies trends in a given time series. The null hypothesis for this test is the absence of a trend. When the null hypothesis is rejected, the alternative hypothesis, which indicates the existence of a trend, is accepted, depending on the level of significance.[54] The Mann-Kendall test provides three key pieces of information:[55]

(i) The Kendall tau or Kendall's rank coefficient, which measures the tendency of the slope. The positive or negative rate reflects an upward or downward trend, respectively. The formula is as follows:

$$Var\ (s) = n(n-1)(2n+5)/18 \quad \text{(IV)}$$

where

$$S = \sum_{j=1}^{j=n-1} \sum_{i=j+1}^{i=n} sign\ (xi - xj) \quad \text{(V)}$$

where

$$\text{sign}\ (xi - xj) = \{1\ if\ (xi - xj) > 0;\ 0\ if\ (xi - xj) = 0;\ -1\ if\ (xi - xj) < 0 \quad \text{(VI)}$$

(ii) Sen's slope represents the overall trend of the time series. It is calculated as the median of the slopes between all possible pairs of points in the series.

$$\beta = Median\left(\frac{xi - xj}{i - j}\right) \forall i < j \quad \text{(VII)}$$

(iii) The significance is determined by the *p*-value, which indicates if the observed trend is statistically significant based on a pre-defined threshold, typically 0.05.

The selection of these methods is related to their robustness and the need for comparability with previous studies. To enhance the value of this work, these methods have been applied to CanESM5 outputs, ensuring that knowledge on heat waves is updated to promote future research.

3. Results

3.1. Analysis of Canadian Earth System Model Version 5 model performance

The performance of CANESM5 was evaluated against the Modern-Era Retrospective analysis for Research and Applications, Version 2, using the KGE and pBias over the 2015 – 2020 period. Figure 2 shows the spatial distribution of KGE values across Senegal. The results show KGE values ranging from 0.24 to 0.78 across all stations included in this study. The model demonstrates good performance, with KGE values exceeding 0.60 at 22 stations in SSP2-2.6, 27 stations in SSP3-4.5, and on 26 stations in SSP5-8.5. At the spatial level, the model performs better in the eastern and central stations of the country, whereas the lowest KGE values are observed in the coastal areas, particularly at the Cap-Kirring station (Figure 2).

The analysis of the KGE is complemented by the pBias, which indicates the percentage of error associated with CANESM5 model output. Figure 3 illustrates the distribution of the pBias values across all stations for the three scenarios selected in this study. The results show that pBias remains below 10% at 34 stations in SSP2-2.6, 39 stations in SSP3-4.5, and on 38 stations in SSP5-8.5. This suggests that the CANESM5 model exhibits good overall behavior, with predictions closely related to observed values. However, positive pBias values indicate a tendency for the model to overestimate the results. The highest biases, ranging from 11 to 17, are observed at the stations of Dakar in the west and Cap Skirring in the south.

3.2. Future evolution of heat waves in Senegal

The future evolution of heat waves was assessed by analyzing the dynamics of the annual 95th percentile

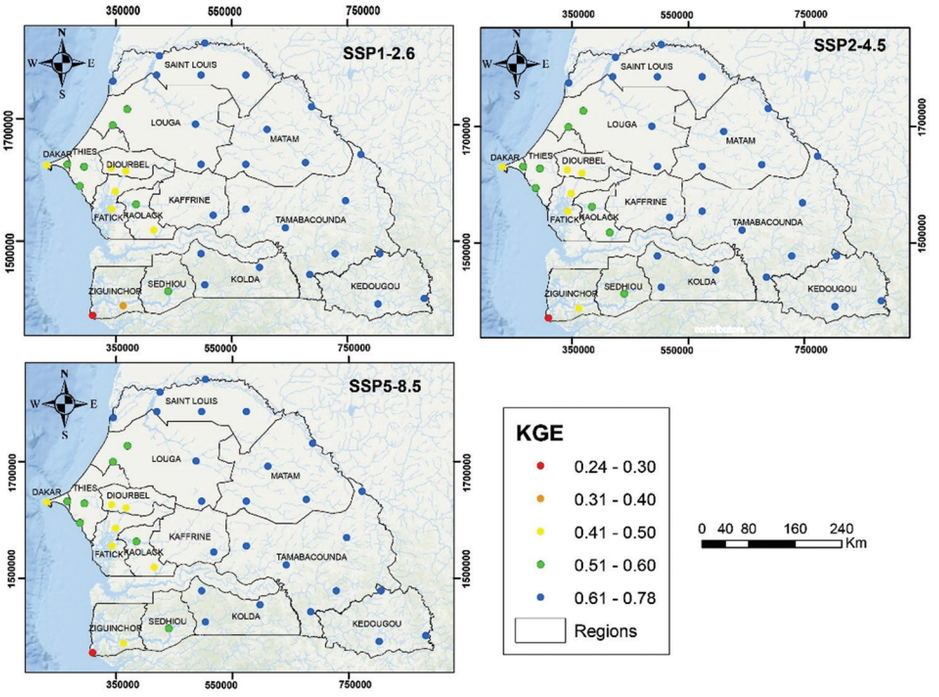

Figure 2. Spatial distribution of KGE values according to different scenarios. Figure created with ArcGis 10.8, Sow and Gaye (2025).

Abbreviations: KGE: Kling-Gupta efficiency; SSP: Shared socioeconomic pathway.

over the period 2020 – 2080. Figure 4 shows the trend in minimum, maximum, and mean temperatures under three climate scenarios (SSP1-2.6, SSP2-4.5, and SSP5-8.5).

The analysis of Figure 4 shows an increase in minimum temperatures across all selected scenarios. In SSP1-2.6, interannual variability is relatively irregular, with temperatures ranging from 28.64°C to 30.34°C. This trend continues in SSP2-4.5, with a slight increase, as temperatures range from 28.66°C to 31.30°C. In contrast, SSP5-8.5 shows a clear interannual variability, marked by a steady increase in

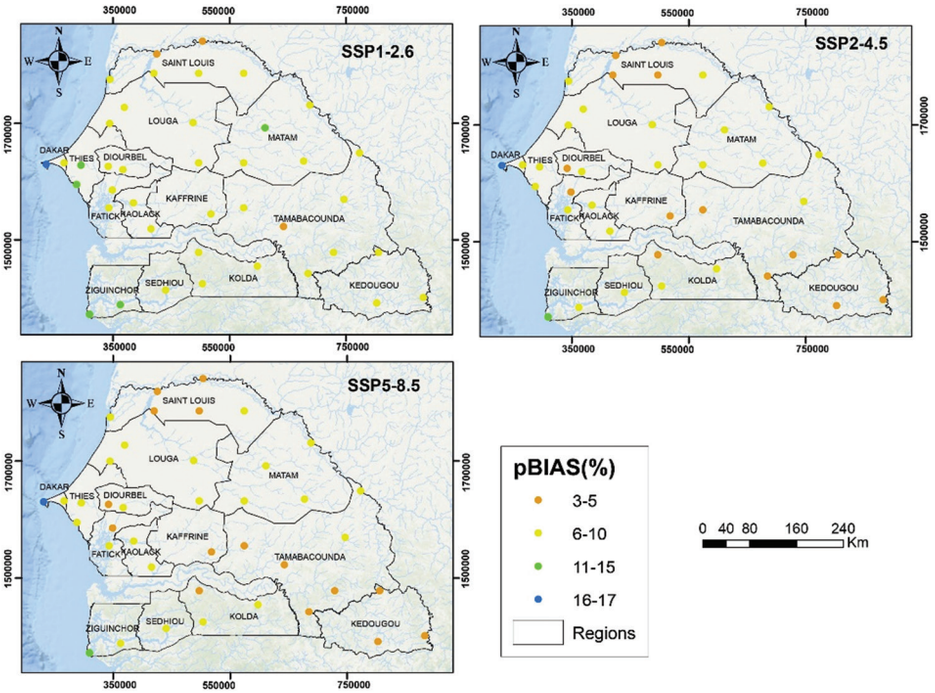

Figure 3. Spatial distribution of pBias values according to the different scenarios. Figure created with ArcGis 10.8, Sow and Gaye (2025).
Abbreviations: pBias: Percent bias; SSP: Shared socioeconomic pathway.

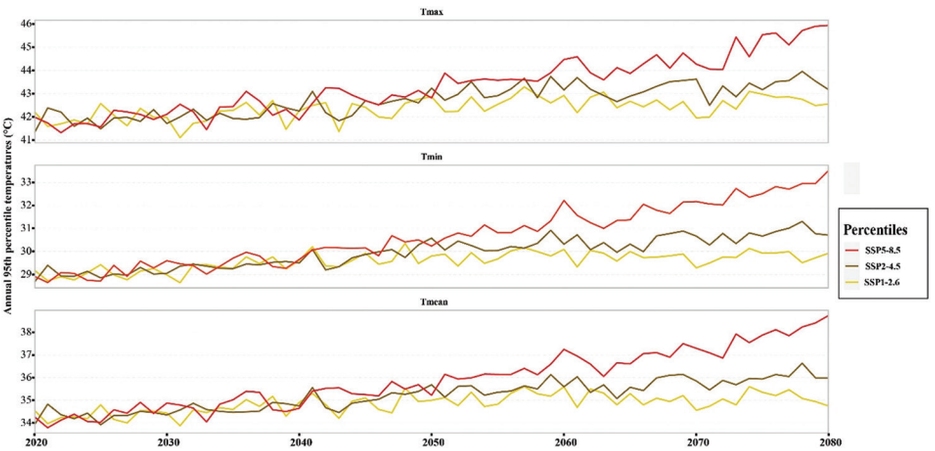

Figure 4. Evolution of the annual 95th percentile of minimum, mean, and maximum temperatures over the period 2020 – 2080. Figure created with ArcGis 10.8, Sow and Gaye (2025).
Abbreviations: SSP: Shared socioeconomic pathway; T_{max}: Maximum temperature; T_{mean}: Mean temperature; T_{min}: Minimum temperature.

the 95th percentile of minimum temperatures over the 2020 – 2080 period.

For mean temperatures, the trend in SSP1-2.6 is similar to that of minimum temperatures, with temperatures ranging from 33.87°C to 35.59°C, a difference of 5.27°C compared to the minimum temperatures in SSP1-2.6. SSP2-4.5 is characterized by a more regular evolution, with mean temperatures ranging from 33.91°C to 36.63°C. This represents an increase of 5.25°C compared to the minimum temperatures in SSP2-4.5. Similarly, SSP5-8.5 shows a steady increase in mean temperatures, ranging from 33.78°C to 38.74°C, with a difference of 5.24°C relative to the corresponding minimum temperature.

Maximum temperatures exhibit a clear warming trend (Figure 4). In SSP1-2.6, temperatures range from 41.09°C to 43.28°C, representing a thermal amplitude of 7.50°C compared to mean temperatures and 12.78° compared to minimum temperatures. SSP2-4.5 shows slightly higher values, ranging from 41.31°C to 43.95°C, with corresponding mean amplitudes of 7.49°C and 12.74°C relative to mean temperatures and minimum temperatures, respectively. SSP5-8.5 reflects a regular increase in extreme temperatures ranging from 41.31°C to 45.93°C, corresponding to a thermal amplitude of 12.67°C relative to minimum temperatures and 7.43°C relative to average temperatures.

In summary, the trend of extreme heat shows a relatively irregular pattern marked by a modest increase up to 2050 for all SSP1-2.6, SSP2-4.5, and SSP5-8.5. However, from 2050 onward, a net warming trend emerges across all variables (Figure 4).

3.3. Spatiotemporal distribution of extreme heat in Senegal

The spatiotemporal distribution of the extreme heat was made based on the average 95th percentile of the 2021 – 2050 and 2051 – 2080 normals.

3.3.1. Spatial distribution of extreme heat from 2021 to 2050

The minimum, maximum, and mean temperatures for three CMIP6 scenarios (SSP1-2.6, SSP2-4.5, and SSP5-8.5) from 2021 to 2050 are presented in Figure 5.

The minimum temperatures are between 28°C and 36°C across all scenarios. Specifically, SSP1-2.6 indicates a minimum temperature between 28°C and 34°C, with most of Senegal falling within the range of 30°C to 32°C. Only a few stations in the Matam region record temperatures exceeding 32°C. SSP2-4.5 reveals a similar pattern with temperatures ranging from 30°C to 32°C across the country. Only Matam stations and part of the Tambacounda and Kedougou regions record temperatures above 32°C. In the SSP5-8.5 scenario, an increase in temperatures is observed compared to the previous scenarios. The temperatures fall between 32°C and 36°C across the country, with the western and central parts of the country fall between 32°C and 34°C. In contrast, the eastern region recorded temperatures between 34°C and 36°C. Administratively, these stations are located primarily in the regions of Kedougou, Tambacounda, Matam, and Saint-Louis.

In addition, temperatures reflect similar spatial dynamics for SSP1-2.6, SSP2-4.5, and SSP5-8.5 (Figure 5). Temperatures range from 32°C to 40°C, with the western-central to southern region recording the lowest values between 32°C and 34°C. In the central and northwestern regions, temperatures range from 34°C to 36°C. The highest mean temperatures are recorded in the central to eastern region of the country, with temperatures ranging from 36°C to 40°C in all scenarios.

Maximum temperatures exhibit the highest values compared to minimum and mean temperatures, ranging from 32°C to 51°C across all three scenarios for the 2021 – 2050 period. SSP1-2.6 presents temperatures between 32°C and 34°C throughout the country, while SSP2-4.5 and SSP5-8.5 show a varied spatial distribution with three temperature classes. In SSP2-4.5, the western region falls between 36°C and 40°C. In the central region, the temperatures range from 40°C to 45°C, and the eastern region presents temperatures between 45°C and 51°C. The distribution in SSP5-8.5 is similar to SSP2-4.5, with the exception at the Ziguinchor station, where temperatures between 34°C and 36°C are observed.

3.3.2. Spatial distribution of heat waves from 2051 to 2080

On the 2051 – 2080 normal (Figure 6), minimum temperatures vary between 28°C and 36°C. In SSP1-2.6, the temperatures are below 32°C across the entire country except the eastern regions of Kedougou, Tambacounda, Matam, and Saint-Louis. In SSP2-4.5, the temperatures fall between 32°C and 34°C across the entire country except south-central stations in the regions of Sedhiou, Kolda, and part of Kaolack and Kaffrine, where the temperatures are below 32°C. For SSP5-8.5, the temperatures range from 32°C to 36°C, with the western and eastern regions showing temperatures ranging from 32°C to 34°C and 34°C to 36°C, respectively.

In addition, mean temperatures show a spatial dynamic that is significantly different compared to

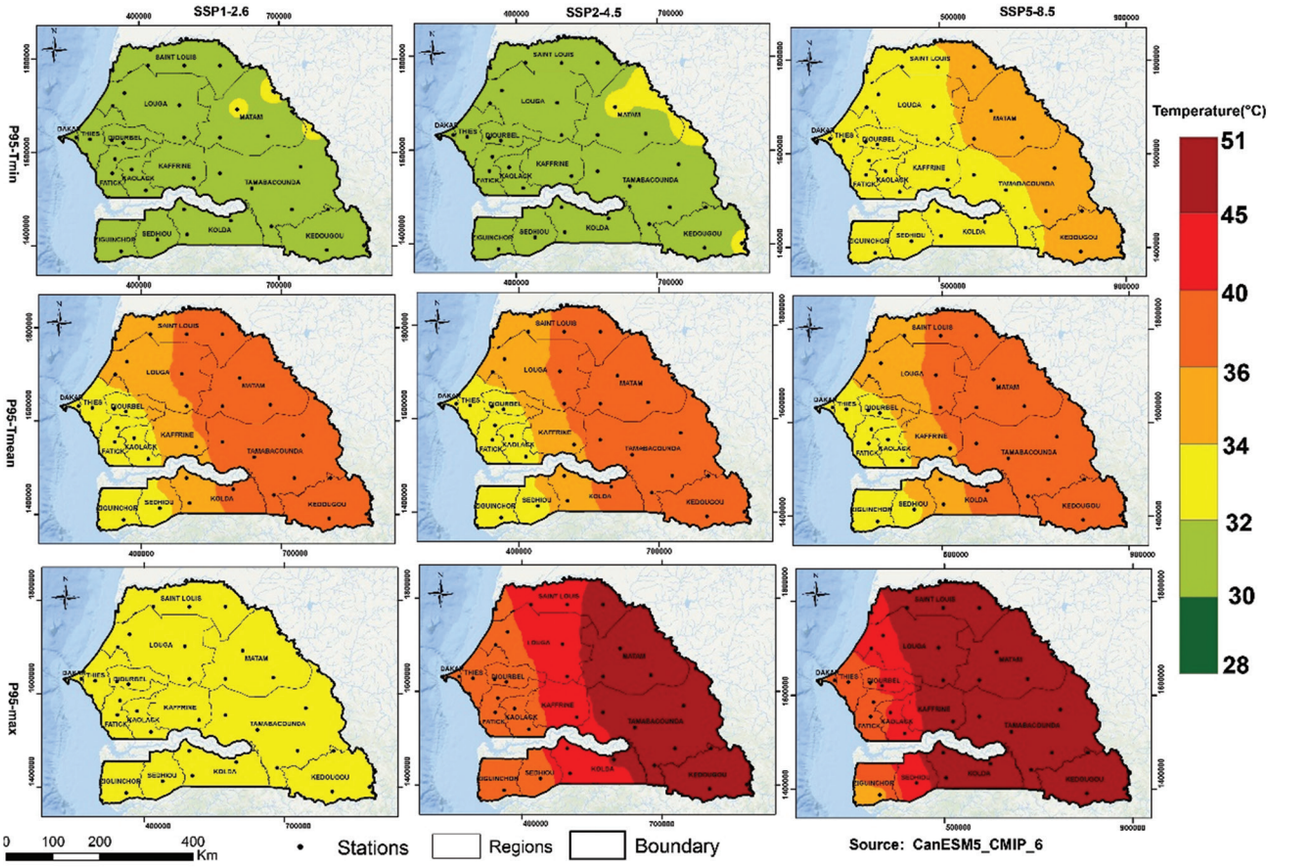

Figure 5. Spatialization of the P95 of T_{min}, T_{mean}, and T_{max} over the period 2021 – 2050. Figure created with ArcGis 10.8, Sow and Gaye (2025).

Abbreviations: P95: 95th Percentile; SSP: Shared socioeconomic pathway; T_{max}: Maximum temperature; T_{mean}: Mean temperature; T_{min}: Minimum temperature.

minimum temperatures, although the observed trend is similar to the mean temperatures in the period 2021 – 2050. A warming trend is observed in the western part of Senegal compared to the earlier period. Mean temperatures vary between 32°C and 40°C, with the western region having the lowest values (32 – 34°C) and the central region where temperatures fall between 34°C and 36°C. The highest temperatures (36 – 40°C) are observed in the eastern region for all three scenarios.

For maximum temperatures, the spatial dynamic is marked by much higher temperatures compared to the minimum and mean temperatures. For SSP1-2.6, the temperatures are between 32°C and 34°C throughout the country, which is similar to the earlier period. In SSP2-4.5 and SSP5-8.5, temperatures range from 40°C to 51°C. The spatial distribution shows noticeable disparities, with the most moderate temperatures observed in the west-central region, while higher temperatures dominate across the rest of the country, with the exception in the coastal regions.

3.4. Interannual variability of extreme heat

3.4.1. Interannual variability of extreme heat from 2021 to 2050

The temporal evolution of the extreme heat from 2021 to 2050 was analyzed using the Lamb anomaly index (Figure 7). The results show a highly irregular interannual pattern of minimum, maximum, and mean temperatures in SSP1-2.6. Two distinct phases can be identified in Figure 7. The first period from 2020 to 2035 is marked by a downward trend in extreme temperatures across all variables, while the second period, from 2035 to 2050, is characterized by an upward trend in extreme heat.

In SSP2-4.5, a highly irregular interannual variability is observed, characterized by alternating phases of rising and falling extreme heat. A declining phase in

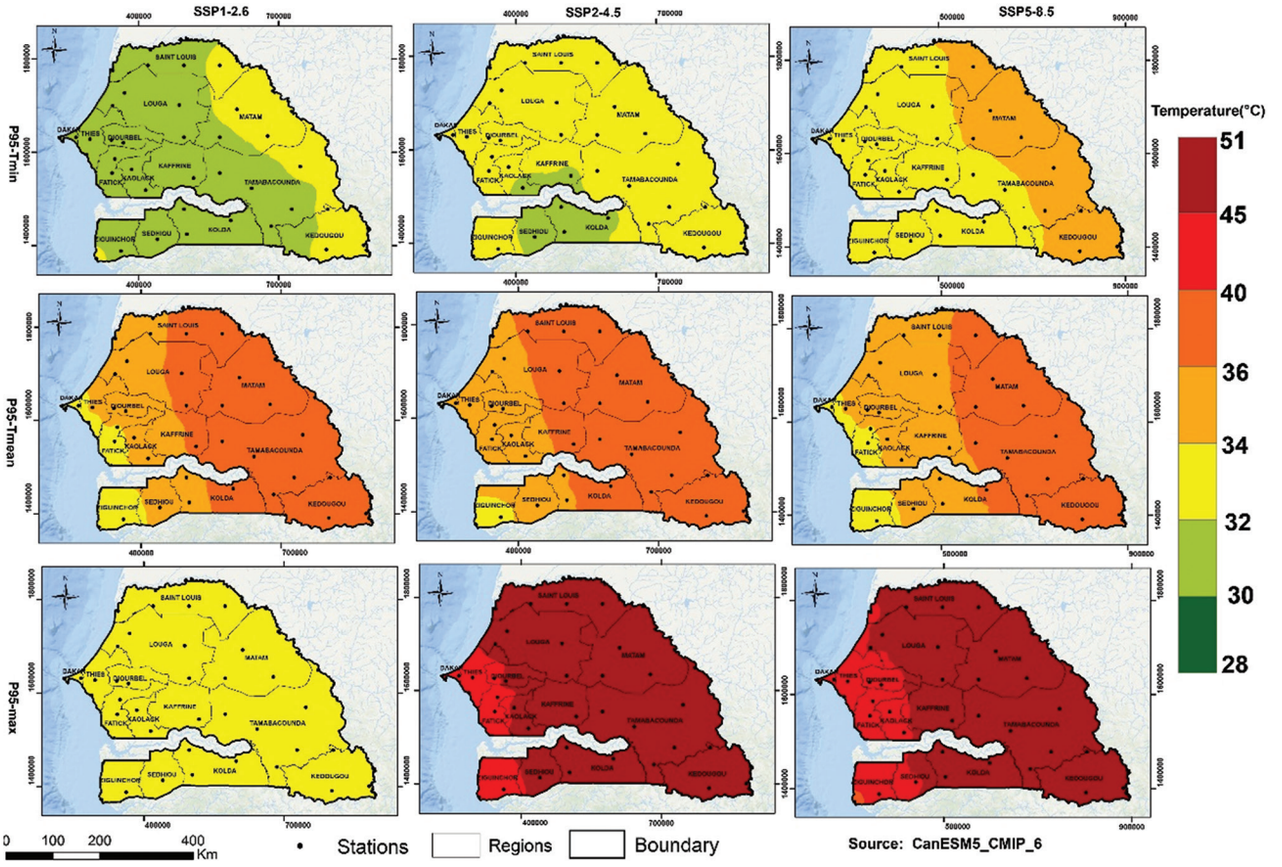

Figure 6. Spatialization of the P95 of T_{min}, T_{mean}, and T_{max} over the period 2051 – 2080. Figure created with ArcGis 10.8, Sow and Gaye (2025).

Abbreviations: P95: 95th Percentile; SSP: Shared socioeconomic pathway; T_{max}: Maximum temperature; T_{mean}: Mean temperature; T_{min}: Minimum temperature.

extreme heat is observed from 2020 to 2040, during which fewer than 5 years show an increase across all three scenarios (SSP1-2.6, SSP2-4.5, and SSP5-8.5). From 2040 onward, the evolution of extreme heat is marked by an overall increase in minimum, maximum, and mean temperatures.

In SSP5-8.5, the diachronic evolution is similar for all temperature variables. There are two phases in the evolution of minimum, maximum, and mean temperatures. From 2021 to 2042, temperatures are marked by a declining trend, with only 5 years being positive in maximum temperatures, four in mean temperatures, and five in minimum temperatures. From 2042 onward, an upward trend emerges across all temperature variables. For minimum temperatures, the projected increases are 0.42°C in SSP1-2.6, 0.69°C in SSP2-4.5, and 0.55°C in SSP5-8.5. In comparison, mean temperatures are expected to rise by 0.25°C, 0.65°C, and 0.41°C in SSP1-2.6, SSP2-4.5, and SSP5-8.5, respectively. Maximum temperatures show increases of 0.035°C for SSP1-2.6, 0.62°C for SSP2-4.5, and 0.45°C for SSP5-8.5.

3.4.2. Interannual variability of extremes from 2051 to 2080

Extreme temperature anomalies were analyzed for the period 2051 – 2080, as shown in Figure 8. This figure shows a pronounced interannual variability in SSP1-2.6 for minimum, maximum, and mean temperatures, with year-to-year fluctuations throughout the period.

SSP2-4.5 is characterized by a more regular trend, though still marked by alternating periods of growth and a decrease in extreme temperatures for all variables. A sustained increase is observed starting from 2068, resulting in positive values of the Lamb anomaly index, except in years 2071 and 2073.

In SSP5-8.5, the period 2051 – 2080 is characterized by low variability on a year-long scale. However,

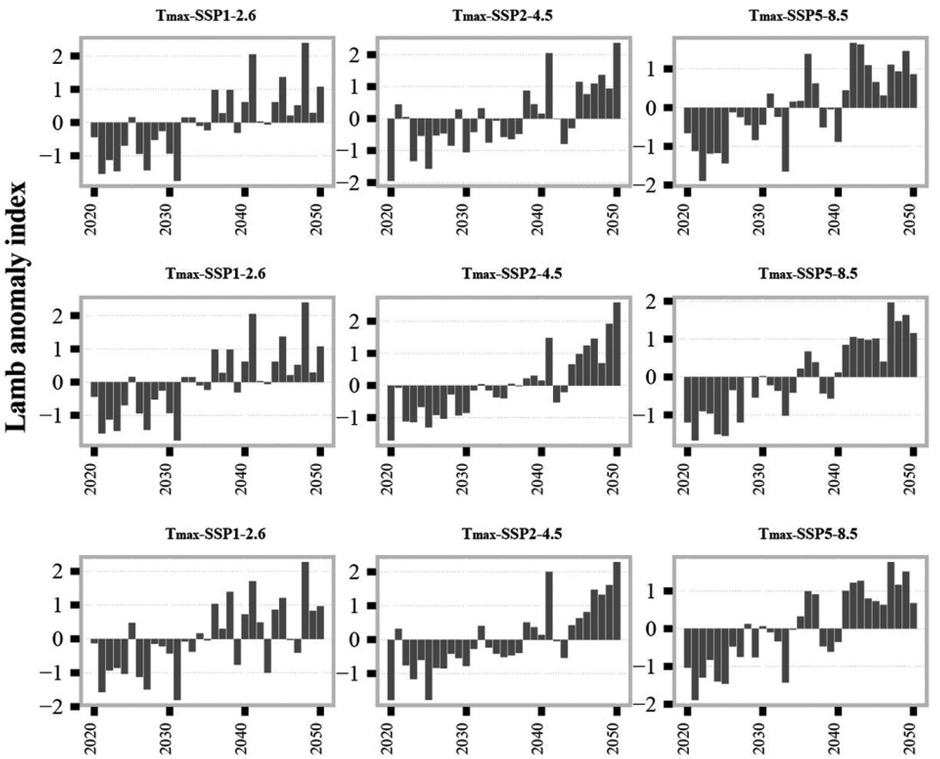

Figure 7. Temporal dynamics of extreme heat over the period 2021 – 2050. Figure created with ArcGis 10.8, Sow and Gaye (2025).

Abbreviations: SSP: Shared socioeconomic pathway; T_{max}: Maximum temperature; T_{mean}: Mean temperature; T_{min}: Minimum temperature.

there are alternating phases of decline and increase in extreme heats. The year 2072 marks a turning point in the evolution of heat waves in Senegal. The first sub-period, from 2050 to 2071, shows a noticeable decrease, followed by an increase from 2072 to 2080. Between these two sub-periods, extreme temperatures (minimum temperatures) increase by 0.07°C in SSP1-2.6, 0.44°C in SSP2-4.5, and 1.35°C in SSP5-8.5. For maximum temperatures, the increase is 0.16°C in SSP1-2.6, 0.23°C in SSP2-4.5, and 1.34°C in SSP5-8.5. For mean temperatures, the increase is 0.05°C in SSP1-2.6, 0.41°C in SSP2-4.5, and 1.34°C in SSP5-8.5.

The diachronic evolution of extreme heat is marked by an interannual variability, characterized by alternating periods of increase and decrease in minimum, maximum, and mean temperatures. The importance of this variability depends on the climate scenarios of this study. Interannual fluctuations are more pronounced in SSP1-2.6 compared to SSP2-4.5. In SSP2-4.5 and SSP5-8.5, the trends are more regular, although fluctuating phases still occur.

3.5. Trend of extreme heat in Senegal

3.5.1. Trends of extreme heat s from 2021 to 2050

The trend of extreme heat in Senegal over the period 2021 – 2050 is analyzed using the Mann–Kendall trend test (Figure 9). The *Z*-value of the test indicates the presence of a trend: a positive value reflects an increase in temperatures over the period, while a negative value indicates a decrease.

Figure 9 shows significant upward trends for minimum temperatures at all stations in all three scenarios (SSP1-2.6, SSP2-4.5, and SSP5-8.5) (p<0.01). For mean temperatures, the warming trends of extreme temperatures are observed with different levels of significance. In SSP1-2.6 and SSP2-4.5, the increase in extreme temperatures is noted with a 99% confidence level (p<0.01), except for west-central, northwest, and northeast in SSP1-2.6 and south of Tambacounda and a Kolda station (SSP2-4.5), for which the significance levels are 95% (p<0.05). An upward trend of minimum temperature is noted in SSP5-8.5 with a significance level of 99% (p<0.01) for all study stations (Figure 9).

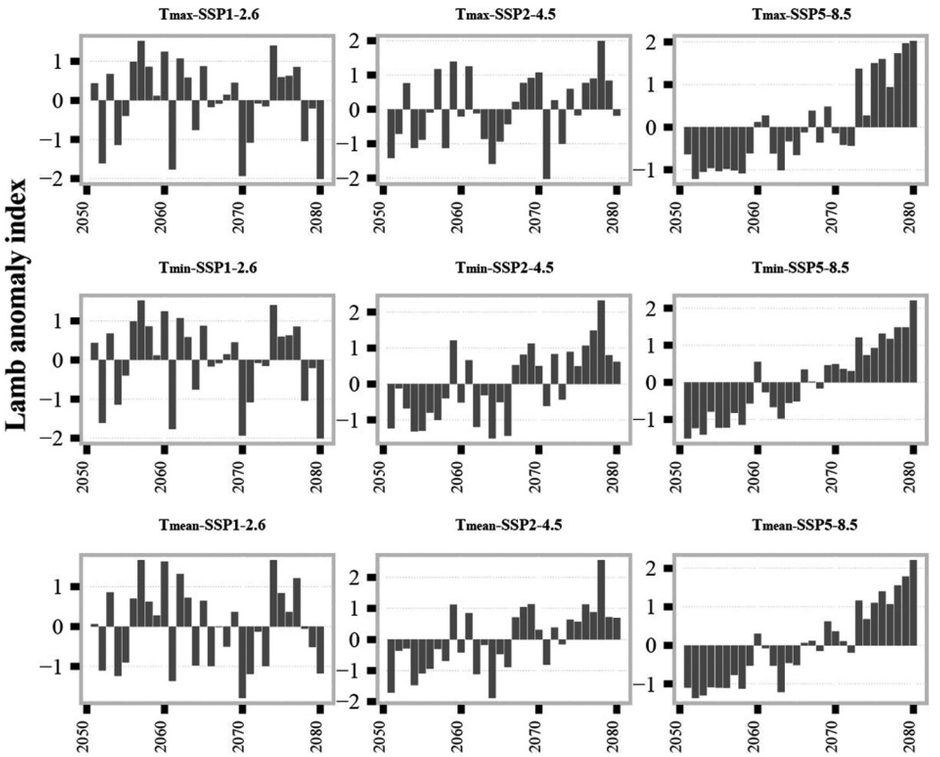

Figure 8. Temporal dynamics of extreme heat over the period 2051 – 2080. Figure created with ArcGis 10.8, Sow and Gaye (2025).

Abbreviations: SSP: Shared socioeconomic pathway; T_{max}: Maximum temperature; T_{mean}: Mean temperature; T_{min}: Minimum temperature.

In addition to the *Z*-value, Sen's slope evaluates the magnitude of the trends. Figure 10 shows the magnitude of the 95th percentile trend of heat waves in Senegal. Minimum temperatures show an upward trend for all scenarios. An average increase of 0.010°C is observed at the Dakar station in SSP1-2.6. For SSP1-2.6 and SSP2-4.5, a temperature increase of between 0.023°C and 0.040°C is noted in the eastern, central, and southwestern regions of the country. For SSP2-4.5, the central and eastern region shows increases in temperatures between 0.040°C and 0.070°C. The growth of extreme heat for SSP5-8.5 follows a similar dynamic with increases in temperatures between 0.040°C and 0.070°C for all study stations.

For mean temperatures, an increase of 0.012°C to 0.030°C is observed in the western regions covering Saint-Louis, Louga, Dakar, Thiès, Fatick, Kaolack, and Ziguinchor for SSP1-2.6 and the south-central (Sedhiou, Kolda, and part of Tambacounda) for SSP2-4.5. For SSP5-8.5, temperature growth ranges from 0.030°C to 0.050°C in western and south-central regions. The eastern region experiences the highest temperature growth between 0.050°C and 0.083°C.

Regarding maximum temperatures, the highest increase between 0.050°C and 0.850°C is only observed at the Mbiddi station (SSP1-2.6) and in parts of Saint-Louis (SSP2-4.5 and SSP5-8.5). The lowest temperature growth is observed in the western region in SSP1-2.6 and in the central region in SSP2-4.5 and SSP5-8.5. The rest of the territory is subject to a moderate increase between 0.030°C and 0.050°C. Thus, a significant spatial variability in temperature growth can be observed across the climate scenarios of this study. In short, the western, south-central, and central regions recorded the lowest temperature growth.

3.5.2. Trends of extreme heat from 2051 to 2080

Figure 11 illustrates the trend of extreme heat over the period 2051 – 2080, which indicates a different trend in SSP1-2.6 for minimum, mean, and maximum temperatures compared to the period 2021 – 2050. Except for the significant temperature growth along the coast and the Kedougou station, the temperature growth is stationary for minimum, mean, and maximum temperatures.

For SSP2-4.5, growth dynamics are observed for minimum and mean temperatures. Spatially, this trend

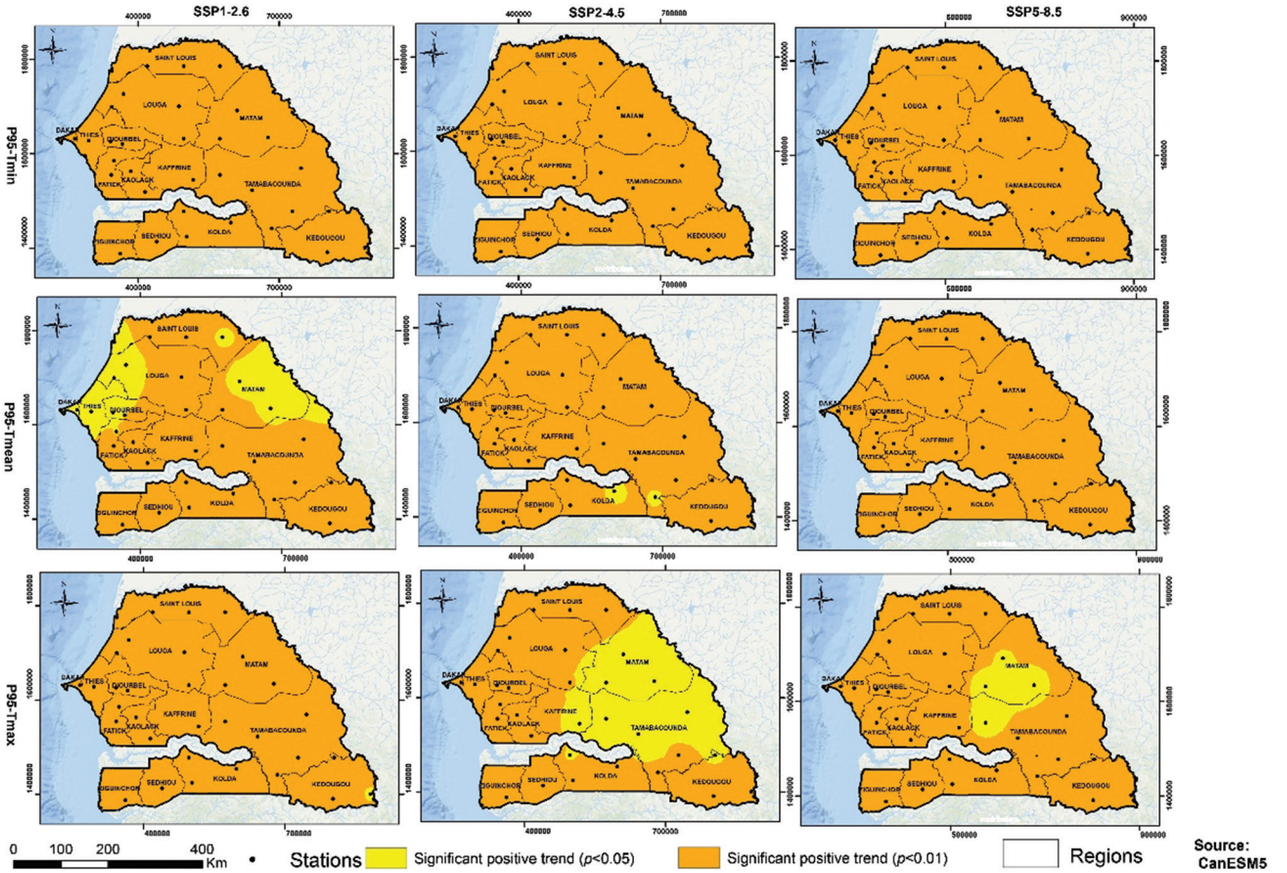

Figure 9. P95 trends of T_{min}, T_{mean}, and T_{max} from 2021 to 2050. Figure created with ArcGis 10.8, Sow and Gaye (2025).

Abbreviations: P95: 95th Percentile; SSP: Shared socioeconomic pathway; T_{max}: Maximum temperature; T_{mean}: Mean temperature; T_{min}: Minimum temperature.

is observed with a 99% significance level (p<0.01) at almost all stations except for those in the northwest region (mean temperatures) and the stations of Saint-Louis, Dagana, and Kedougou (minimum temperatures), which the significance levels are 95% (p<0.05).

A significant warming trend is observed in SSP5-8.5 at a 99% significance level (p<0.01) for minimum and mean temperatures, while a stationary trend is observed for maximum temperatures at all stations.

In addition, Sen's slope for the period 2051 – 2080 shows the magnitude of the temperature trend. Figure 12 illustrates Sen's slope results from the Mann–Kendall test for the period 2051 – 2080, based on data from the 40 stations included in this study.

An increase in minimum temperatures between 0.010°C and 0.030°C is observed in SSP1-2.6 and the western region of SSP2-4.5 (Figure 12). The eastern region of SSP2-4.5 shows an increase of minimum temperatures between 0.030°C and 0.050°C. SSP5-8.5 records the largest increase in minimum temperatures above 0.050°C.

The magnitude of the Sen's slope of mean temperatures is irregular. The temperature growth in SSP1-2.6 is between 0.030°C and 0.050°C at all stations in this study. A decrease in temperature growth (below 0.030°C) is observed in SSP2-4.5 throughout Senegal, except for the regions in Matam and Tambacounda, where the temperature growth falls between 0.030°C and 0.050°C. In SSP5-8.5, the temperature increase ranges from 0.013°C to 0.068°C. The highest increase in temperatures between 0.050°C and 0.068°C is observed in the eastern, northern, and central regions. A moderate temperature growth between 0.030°C and 0.050°C is observed in southwestern (Ziguinchor, Sedhiou, and Kolda), central (Fatick, Kaolack, Kaffrine, and Diourbel), and western (Dakar, Thiès, and parts of Saint-Louis and Louga) regions.

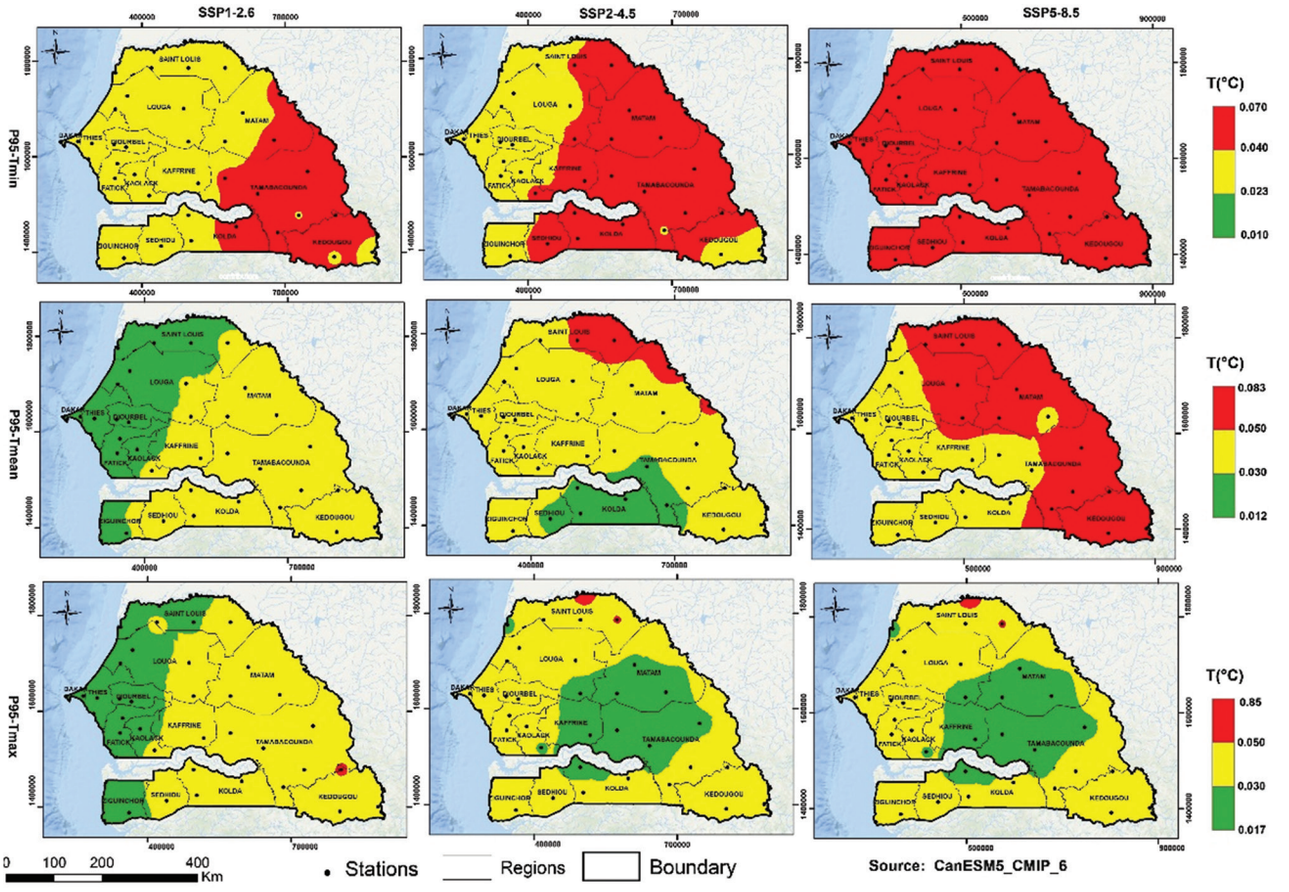

Figure 10. Distribution of the Sen's slope in Senegal from 2021 to 2050. Figure created with ArcGis 10.8, Sow and Gaye (2025).

Abbreviations: P95: 95th Percentile; SSP: Shared socioeconomic pathway; T: Temperature; T_{max}: Maximum temperature; T_{mean}: Mean temperature; T_{min}: Minimum temperature.

Regarding maximum temperatures, all stations in this study exhibit notably low increases, with values below 0.050°C in SSP1-2.6. At the spatial level, only the western region recorded the largest increase between 0.030°C and 0.050°C. The temperature increases in other regions are below 0.030°C. The recorded increases of temperatures at all stations in SSP2-4.5 and SSP-8.5 are below 0.030°C.

4. Discussion

The purpose of this work was to study the future trends of minimum, maximum, and mean temperatures over two climate normals (2021 – 2050 and 2051 – 2080). Three CanESM5 scenarios (SSP1-2.6, SSP2-4.5, and SSP5-8.5) were studied at 40 stations.

The results of this study reflect an increase in temperatures across all variables at the national level. This upward trend is observed in minimum, mean, and maximum temperatures in SSP1-2.6, SSP2-4.5, and SSP5-8.5. The warming dynamic is the greatest in SSP5-8.5. This trend aligns with the work of the Intergovernmental Panel on Climate Change (IPCC),[5] which predicted an increase in temperatures. Previous studies from Perkins *et al.*[7] and Das and Umamahesh[6] showed that the increase in temperatures would result in a strengthening of global extreme heat toward the end of the 21st century. At the Sahelian scale, Ringard *et al.*[9] reported similar findings regarding the intensification of extreme heat. In Senegal, Sagna *et al.*[56] support the IPCC's predictions by confirming this warming trend.

The results show an overall upward trend across all stations, scenarios, and temperature variables for the period 2021 – 2050. In contrast, for the period 2051 – 2080, continental stations in SSP1-2.6 for minimum and mean temperatures and all scenarios for maximum temperatures display a stationary trend. This overall upward trend is supported by the work of

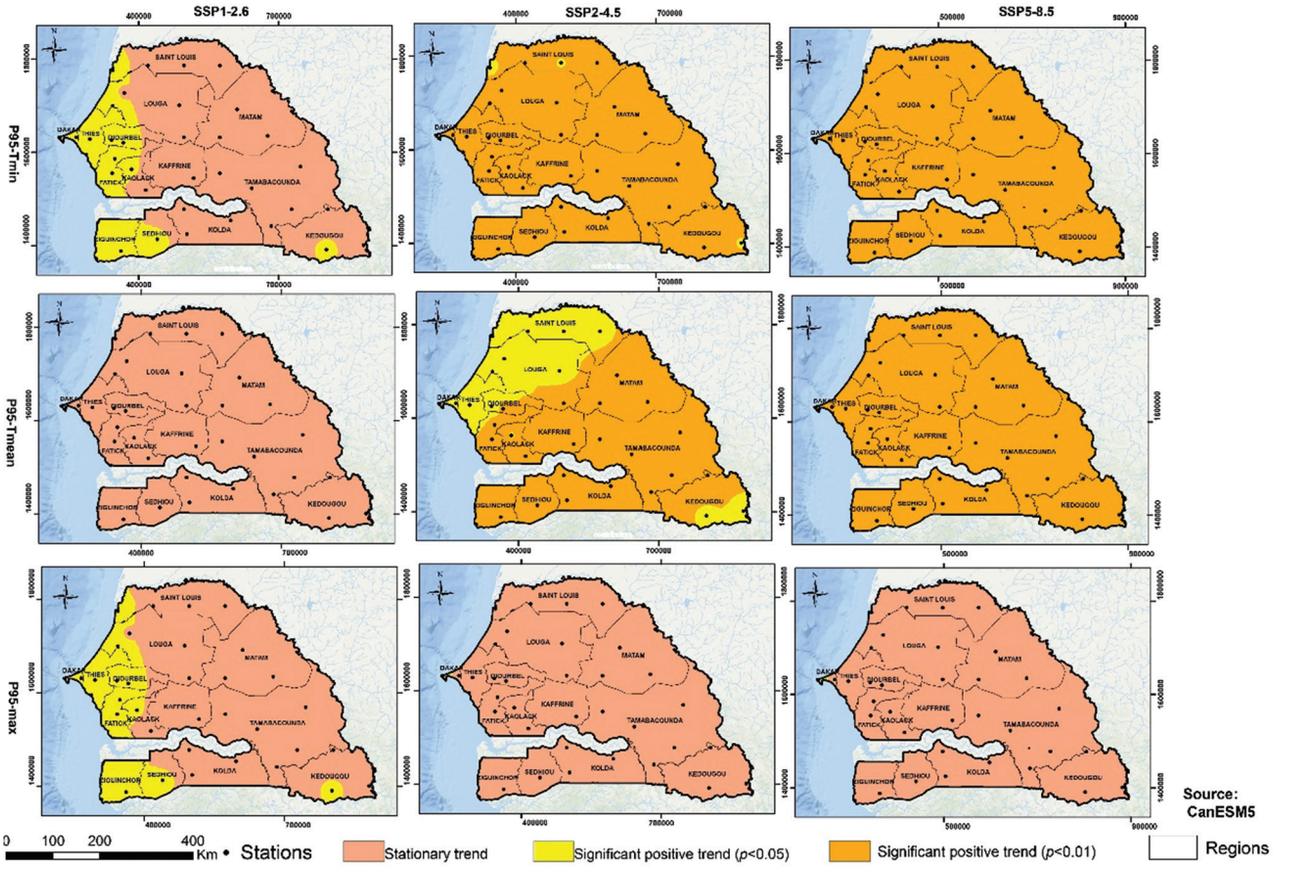

Figure 11. P95 trends of T_{min}, T_{mean}, and T_{max} from 2051 to 2080. Created with ArcGis 10.8, Sow and Gaye (2025).

Abbreviations: P95: 95th Percentile; SSP: Shared socioeconomic pathway; T_{max}: Maximum temperature; T_{mean}: Mean temperature; T_{min}: Minimum temperature.

Ringard,[57] which predicted a warming of temperatures in the future. The dynamics of extreme heat in Senegal can be explained by the combination of climatic and geographical factors. One factor contributing to the persistence of heat conditions is the influence of subtropical and Saharan-Libyan high-pressure systems. These systems lead to the convergence of hot and dry air masses from the Sahara toward the Sahel, creating favorable conditions for atmospheric blocking, which increases the likelihood of extreme heat.[22] In addition, the atmospheric influences are combined with the low humidity level and low cloud cover in these regions, further contributing to the intensification of heat waves.

In addition, the trend is characterized by a greater increase in the minimum temperatures, which is reflected in the reduction of thermal amplitudes. This is likely linked to the effects of human activities, particularly greenhouse gas emissions.[58] Specifically, CO_2 emission from the Earth's surface at night constrains nocturnal cooling. Furthermore, artificial or desert surfaces with a high thermal capacity and conductivity trap heat during the day, which is released at night, further inhibiting cooling. These factors could explain the faster rise in minimum temperatures compared to mean and maximum temperatures observed in Senegal. These findings extend the results of Braganza *et al*.,[59] Easterling *et al*.,[60] and Hartmann *et al.*[61] regarding the faster increase in minimum temperatures globally, as well as the studies of Trigo *et al*.,[62] Ringard,[57] Rome *et al*.,[63] and Barbier[64] in Africa and the Sahel. The increasing trend of minimum temperatures underscores the severity of heat waves, as highlighted by Meehl and Tebaldi[65] and Trigo *et al.*[62]

The spatial dynamics of these trends indicate an increase in extreme temperatures moving eastward. This is due to geographical factors such as high humidity and elevated hydrometric levels in coastal regions compared to inland regions. This spatial distribution of extreme

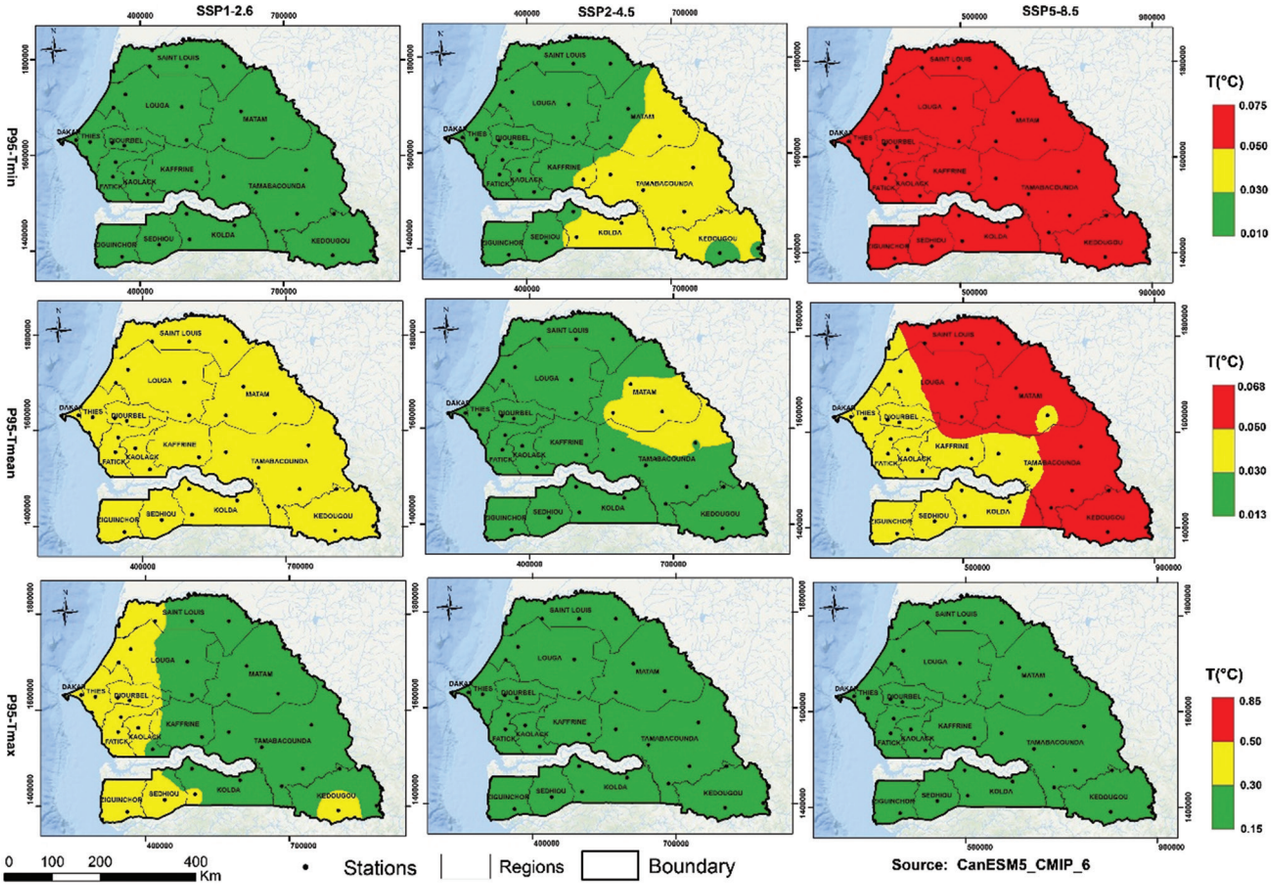

Figure 12. Distribution of the Sen's slope in Senegal from 2051 to 2080. Created with ArcGis 10.8, Sow and Gaye (2025).

Abbreviations: P95: 95th Percentile; SSP: Shared socioeconomic pathway; T: Temperature; T_{max}: Maximum temperature; T_{mean}: Mean temperature; T_{min}: Minimum temperature.

temperatures supports the work of Ndiaye *et al*.,[30] which characterized the spatial dynamics of temperatures at the national scale in Senegal.

Thus, this work projected the future evolution of extreme heat for the periods 2051 – 2080 and 2051 – 2080 with an upward trend across all scenarios. A comparative analysis of extreme temperature trends using different outputs of CMIP6 would be a relevant direction for future studies.

5. Conclusion

This study aimed to analyze the evolution and future trends of heat waves over the periods 2021 – 2050 and 2051 – 2080. The data from the CanESM5 model were resampled and extracted based on the coordinates of 40 stations selected for this study. Minimum, mean, and maximum temperatures were examined under three scenarios (SSP1-2.6, SSP2-4.5, and SSP5-8.5) of CMIP6. The study was performed through the spatialization of extremes using IDW, the analysis of interannual variability using the Lamb index, and trend detection using the Mann-Kendall test.

The observed dynamics of minimum temperatures range from 28°C to 36°C across all scenarios. In SSP1-2.6, almost the entire country shows dynamics of minimum temperatures below 32°C, particularly in the western region. In SSP2-4.5, minimum temperatures range from 32°C to 34°C nearly across the entire territory, while temperatures below 32°C are noted at the stations in the south-central region. In SSP5-8.5, minimum temperatures exceed 32°C across all stations but remain below 36°C. In addition, mean temperatures range from 32°C to 40°C with similar patterns across all scenarios. The lowest values (32°C – 34°C) are observed in the western region, while the central region shows moderate values (34°C – 36°C). Elevated mean temperatures

(36°C – 40°C) are observed in the eastern region. The maximum temperatures are marked by the highest spatial dynamic across all temperature variables. In SSP1-2.6, maximum temperatures fall between 32°C and 34°C across Senegal. For SSP2-4.5 and SSP5-8.5, maximum temperatures range from 40°C to 51°C. In addition, the Lamb anomaly index indicates a greater increase in minimum temperatures with an increase of 0.43°C in SS1-2.6, 1.06°C in SSP2-4.5, and 2.18°C in SSP5-8.5. The increases of maximum temperatures in SSP1-2.6, SSP2-4.5, and SSP5-8.5 are 0.50°C, 1.05°C, and 2.03°C, respectively, while mean temperatures increased by 0.48°C in SSP1-2.6, 1.04°C in SSP2-4.5, and 2.16°C for SSP5-8.5.

The results obtained reflect an upward trend in extreme heat in all variables, scenarios, and stations. However, the increase is more significant in the first period (2021 – 2050) than in the second (2051 – 2080). At the spatial level, the western region showed the lowest increment of below 0.030°C, while the remaining regions in Senegal are experiencing greater increases that exceed 0.050°C in the first period.

In short, this study analyzed the trend and future evolution of extreme heat in terms of minimum, mean, and maximum temperatures for the periods 2021 – 2050 and 2051 – 2080. Data from the CanESM5 model were used in SSP1-2.6, SSP2-4.5, and SSP5-8.5. In light of these results, it is necessary to study the future trend of heat waves using other CMIP6 models.

Acknowledgments

None.

Funding

None.

Conflict of interest

The authors declare no conflicts of interest.

Author contributions

Conceptualization: All authors
Formal analysis: All authors
Methodology: Moussa Sow
Software: Moussa Sow
Validation: Moussa Sow, Demba Gaye
Writing – original draft: Moussa Sow
Writing–review & editing: Demba Gaye

Availability of data

The data used in this article have been cited in the document. The links to access the data have been shared in-text.

References

1. Costello A, Abbasb M, Allen A, *et al*. Managing the health effects of climate change: Lancet and University College London Institute for Global Health Commission. *Lancet*. 2009;373(9676):1693-1733. doi: 10.1016/s0140-6736(09)60935-1
2. IPCC. *Climate Change 2014: Synthesis Report. Contribution of Working Groups I, II and III*. Geneva, Switzerland; 2014. Available from: https://www.ipcc.ch/site/assets/uploads/2018/05/SYR_AR5_FINAL_full_wcover.pdf [Last accessed on 2025 Mar 15].
3. Sharma A, Goyal MK. Assessment of the changes in precipitation and temperature in Teesta River basin in Indian Himalayan Region under climate change. *Atmos Res*. 2019;231:104670. doi: 10.1016/j.atmosres.2019.104670
4. Chen H, Zhao L, Cheng L, *et al*. Projections of heatwave-attributable mortality under climate change and future population scenarios in China. *Lancet Reg Health West Pac*. 2022;28:100582. doi: 10.1016/j.lanwpc.2022.100582
5. IPCC. *Summary for Policymakers. In Climate Change 2013: The Physical Science Basis. Contribution of Working Group I*. Cambridge, United Kingdom and New York, NY, USA: Cambridge University Press; 2013. Available from: https://www.ipcc.ch/site/assets/uploads/2018/03/wg1ar5_summaryvolume_final.pdf [Last accessed on 2025 Mar 17].
6. Das J, Umamahesh NV. Heat wave magnitude over India under changing climate: Projections from CMIP5 and CMIP6 experiments. *Int J Clim*. 2021;42(1):331-351. doi: 10.1002/joc.7246
7. Perkins SE, Alexander LV, Nairn JR. Increasing frequency, intensity and duration of observed global heatwaves and warm spells. *Geophys Res Lett.* 2012;39:L20714. doi: 10.1029/2012GL053361
8. Zeng Q, Li GX, Cui YS, Jiang GH, Pan XC. Estimating temperature-mortality exposure-response relationships and optimum ambient temperature at the multicity level of China. *Int J Environ Res Public Health*. 2016;13(3):279.
9. Ringard J, Dieppois B, Rome S, *et al*. *Evolution des pics de Températures en Afrique de l'Ouest: Étude comparative entre Abidjan et Niamey*. p. 231-237. Available from: https://www.researchgate.net/publication/260176381_evolution_des_pics_de_temperatures_en_afrique_de_l'ouest_etude_comparative_entre_abidjan_et_niamey [Last accessed

on 2025 Mar 15].
10. World Meteorological Organization and World Health Organization. *Heat Waves and Health: Guidance on Warning-System Development*. *WMO-No*; 2015. Available from: https://cdn.who.int/media/docs/default-source/climate-change/heat-waves-and-health---guidance-on-warning-system-development.pdf?sfvrsn=e4813084_2&download=true [Last accessed on 2025 Mar 12].
11. Watts N, Adger WN, Agnolucci P, *et al*. Health and climate change: Policy responses to protect public health. *Lancet*. 2015;386(10006):1861-1914. doi: 10.1016/s0140-6736(15)60854-6
12. World Health Organization. *World Health Statistics 2017: Monitoring Health for the SDGs, Sustainable Development Goals*. WHO; 2017. Available from: https://iris.who.int/bitstream/handle/10665/255336/9789241565486-eng.pdf?sequence=1&isAllowed=y [Last accessed on 2025 Mar 12].
13. FAO. *L'impact des Catastrophes Sur L'agriculture et la Sécurité Alimentaire Prévenir et Réduire Les Pertes En Investissant Dans la Résili*ence; 2023. Available from: https://openknowledge.fao.org/server/api/core/bitstreams/2580a391-043a-45c8-9537-3eb7f8b485fe/content [Last accessed on 2025 Mar 17].
14. Lobell DB, Burke MB, Tebaldi C, Mastrandrea MD, Falcon WP, Naylor RL. Prioritizing climate change adaptation needs for food security in 2030. *Science.* 2008;319(5863):607610. doi: 10.1126/science.1152339
15. Chakraborty DS, Tiedemann A, Teng P. Climate change: Potential impact on plant disease. *Environ Pollut.* 2000;108:317326. doi: 10.1016/S0269-7491(99)00210-9
16. Diouf NS. *Évolution Spatio-temporelle des Vagues de Chaleur en Afrique de l'Ouest et Risques Sanitaires Associes. Mémoire de Master, Physiques et Applications, Sciences de l'Atmosphère et de l'Ocean.UASZ*; 2018. Available from: https://rivieresdusud.uasz.sn/xmlui/bitstream/handle/123456789/955/diouf_memoire_2018.pdf?sequence=1&isAllowed=y [Last accessed on 2025 Mar 08].
17. Bodian A, Diop L, Panthou G, *et al*. Recent trend in hydroclimatic conditions in the senegal river basin. *Water*. 2020;12(2):436. doi: 10.3390/w12020436
18. Ndiaye PM. *Evaluation, Calibration et Analyse des Tendances Actuelles et Futures de L'évapotranspiration de Référence dans le Bassin du FLEUVE SÉNÉGAL*. UGB; 2021. Available from: https://cda-omvs.org/wp-content/uploads/2016/06/13680_evaluation-calibration-et-analyse-des-tendances-actuelles-et-futures-evapotranspirations-BFS.pdf [Last accessed on 2025 Mar 08].
19. Eyring V, Bony S, Meehl GA, *et al*. Overview of the coupled model intercomparison project phase 6 (CMIP6) experimental design and organisation. *Geosci Model Dev Disc.* 2016;9(5):1937-1958. doi: 10.5194/gmd-9-1937-2016
20. Hirsch AL, Ridder NN, Perkins-Kirkpatrick SE, Ukkola A. CMIP6 multimodel evaluation of present-day heatwave attributes. *Geophys Res Lett*. 2021;48:1-11. doi: 10.1029/2021GL095161
21. Toure M, Thiaw WM, Sy I, *et al*. Machine learning-based prediction of heatwave-related hospitalizations: A case study in Matam, Senegal. *Public Health*. 2025;3:1-26. doi: 10.20944/preprints202503.1797.v1
22. Sow M, Gaye D, Diakhate MM. Analysis of the spatiotemporal evolution of the trend of extreme heat in Senegal. *Vertigo.* 2024;24(2):1-21. doi: 10.4000/12jq1
23. Sow M, Gaye D, Diakhate MM. Analysis of the spatiotemporal evolution of the trend of extreme heat in Senegal. *Vertig*o. 2024;24(2):1-21. doi: 10.4000/12jq1
24. Sow M, Gaye D. Categorization and multi-criteria analysis of heat wave vulnerability in Senegal. *J Water Clim Change.* 2024;15(11):53825396. doi: 10.2166/wcc.2024.090
25. Sy I, Cissé B, Ndao B, *et al*. Heat waves and health risks in the northern part of Senegal: Analysing the distribution of temperature-related diseases and associated risk factors. *Environ Sci Pollut Res*. 2022;29(55):8336583377. doi: 10.1007/s11356-022-21205-x
26. Gaye AT, Lo HM, Sakho-Djimbira S, Fall MS, Ndiaye I. *Senegal: Revue du contexte Socioeconomique, Politique et Environnemental*. IED, PRESA; 2015. Available from: https://www.iedafrique.org/img/pdf/revue_resilience_croissance_et_changement_climatique_au_senegal-2.pdf [Last accessed on 2025 Mar 15].
27. Wade CT, Toure O, Diop M. *Gestion des Risques Climatiques*. IED, PRESA; 2015. Available from: https://www.iedafrique.org/img/pdf/revue_thematique_2015.pdf [Last accessed on 2025 Mar 15].
28. Bodian A. Characterization of recent temporal variability of annual rainfall in Senegal (West Africa). *Physio Geo Environ.* 2014;8:297-312. doi: 10.4000/physio-geo.4243
29. Yade M, Sagna P, Sambou P. *Migrations de l'Equateur Meteorologique et Precipitations au Senegal en 2008 et 2009. 25ème Colloque Ass Int de Cli*. p. 781-786. Available from: https://www.researchgate.net/publication/331232160_migrations_de_l'equateur_meteorologique_et_precipitations_au_senegal_en_2008_et_2009 [Last accessed on 2025 Mar 12].
30. Ndiaye PM, Gaye D, Sow SA. Spatio-temporal characterization and analysis of temperature trends in Senegal. *Eur Sci J.* 2020;16(33):105-121. doi: 10.19044/esj.2020.v16n33p105
31. Bigot S, Dumas D, Brou YT, *et al*. Projections climatiques

CMIP6 à l'echelle du sud-est de la cote d'ivoire: Evolution des contraintes thermo-pluviometriques pour les principaux Agrosystèmes associant cacao, hevea, palmier à huile et manioc. *Conference: 35ème Colloque Annuel de l'Association Internationale de Climatologie – AIC 2022At: Toulouse;* 2022. p. 60-66. Available from: https://agritrop.cirad.fr/606582/1/ID606582.pdf [Last accessed on 2025 Mar 08].

32. Mmame B, Ngongondo C. Evaluation of CMIP6 model skills in simulating tropical climate extremes over Malawi, Southern Africa. *Model Earth Syst Environ.* 2024;10(2):16951709. doi: 10.1007/s40808-023-01867-3
33. Wang D, Xu T, Fang G, *et al*. Characteristics of marine heatwaves in the Japan/East Sea. *Remote Sens*. 2022;14(4):936. doi: 10.3390/rs14040936
34. Ajibola FO, Zhou B, Shahid S, Ali MA. Performance of CMIP6 HighResMIP simulations on West African Drought. *Front Earth Sci.* 2022;10:925358. doi: 10.3389/feart.2022.925358
35. Akinsanola AA, Kooperman GJ, Pendergrass AG, Hannah WM, Reed KA. Seasonal representation of extreme precipitation indices over the United States in CMIP6 present-day simulations. *Environ Res Lett.* 2020;15(9):094003. doi: 10.1088/1748-9326/ab92c1
36. Ha K, Moon S, Timmermann A, Kim D. Future changes of summer monsoon characteristics and evaporative demand over Asia in CMIP6 simulations. *Geophys Res Lett*. 2020;47(8):e2020GL087492. doi: 10.1029/2020GL087492
37. Jeong DI, Cannon AJ, Yu B. Influences of atmospheric blocking on North American summer heatwaves in a changing climate: A comparison of two Canadian Earth system model large ensembles. *Clin Change.* 2022;172(5):1-21. doi: 10.1007/s10584-022-03358-3#citeas
38. Neal E, Huang CS, Nakamura N. The 2021 Pacific Northwest heat wave and associated blocking: Meteorology and the role of an upstream cyclone as a diabatic source of wave activity. *Geophys Res Lett.* 2022;49(8):e2021GL097699. doi: 10.1029/2021GL097699
39. Arora VK, Scinocca JF, Boer GJ, *et al*. Carbon emission limits required to satisfy future representative concentration pathways of greenhouse gases. *Geophys Res Lett.* 2011;38(5):1-6. doi: 10.1029/2010GL046270
40. Brunner L, Schaller N, Anstey J, Sillmann J, Steiner AK. Dependence of present and future European temperature extremes on the location of atmospheric blocking. *Geophys Res Lett.* 2018;45(12):6311-6320. doi: 10.1029/2018GL077837
41. Schaller N, Sillmann J, Anstey J, Fischer EM, Grams CM, Russo S. Influence of blocking on Northern European and Western Russian heatwaves in large climate model ensembles. *Environ Res Lett.* 2018;13(5):054015. doi: 10.1088/1748-9326/aaba55
42. Dehban H, Zareian MJ, Gohari A. Evaluating regional climate change during 2021-2080 for Iran and neighboring countries (a comparative analysis of projections and reanalysis data). *Theor Appl Climatol.* 2025;156:143. doi: 10.1007/s00704-025-05381-7
43. Zareian MJ, Dehban H, Gohari A, Torabi HA. Assessment of CMIP6 models performance in simulation precipitation and temperature over Iran and surrounding regions. *Environ Monit Assess.* 2024;196:701. doi: 10.1007/s10661-024-12878-7
44. Da Silva ASA, Stosic B, Menezes RSC, Singh VP. Comparison of interpolation methods for spatial distribution of monthly precipitation in the State of Pernambuco, Brazil. *J Hydrol Eng.* 2019;24:3. doi: 10.1061/(ASCE)HE.1943-5584.0001743
45. Teegavarapu RSV, Meskele T, Pathak CS. Geo-spatial grid-based transformations of precipitation estimates using spatial interpolation methods. *Comp Geosci.* 2012;40:2839. doi: 10.1016/j.cageo.2011.07.004
46. Jones PA *User's Guide for SCRIP: A Spherical Coordinate Remapping and Interpolation Package, Version 1.4. The Regents of the University of California*. Available from: https://oasis.cerfacs.fr/wp-content/uploads/sites/114/2021/03/globc_scripusers_1998.pdf [Last accessed on 2025 Mar 15].
47. Kim KH, Shim PS, Shin S. An alternative bilinear interpolation method between spherical grids. *Atmosphere.* 2019;10(3):123. doi: 10.3390/atmos10030123
48. Goudiaby O, Bodian A, Dezetter A, Diouf I, Ogilvie A. Evaluation of gridded rainfall products in three West African Basins. *Hydrology*. 2024;11(6):75. doi: 10.3390/hydrology11060075
49. Bodian A, Ndiaye PM, Diop SB, *et al*. Evaluation and calibration of alternative methods for estimating reference evapotranspiration in the main hydrosystems of Senegal: Senegal, Gambia and Casamance River Basins. *Proc IAHS*. 2024;385:415421. doi: 10.5194/piahs-385-415-2024
50. Saley MB, Tanoh R, Kouame KF, *et al*. *Variabilite Spatio-temporelle de la Pluviometrie et son Impact Sur les Ressources En Eaux Souterraines: Cas du district d'Abidjan (Sud de la Côte d'Ivoire)*. University de Cocody; 2009. Available from: https://www.sifee.org/client_file/upload/colloques%20documentation/2009%20niamey/3_saley_comm.pdf [Last accessed on 2025 Mar 12].
51. Faye C, Ba Djibrirou D, Diedhiou SO. The anomaly of the minimum and maximum temperature in the

south-eastern part of Senegal. *J Sci Res Univ Lome.* 2019;21(4-1):27-37.
doi: 10.12691/ajfn-13-2-2

52. Kendall MG. *Rank Correlation Methods*. 4th ed. London, U.K: Charles Griffin; 1975.
53. Mann HB. Nonparametric tests against trend. *Econometrica.* 1945;13:245-259.
doi: 10.2307/1907187
54. Braud I. *Methodologies D'analyse de Tendances sur de Longues Series Hydrometeorologiques*. Fiche Technique Othu N 2; 2011. Available from: https://hal.inrae.fr/hal-02595255v1/document [Last accessed on 2025 Mar 08].
55. Ringard J, Chiriaco M, Bastin S, Habets F. Recent trends in climate variability at the local scale using 40 years of observations: The case of the Paris region of France. *Atmos Chem Phys.* 2019;19(20):13129-13155.
doi: 10.5194/acp-19-13129-2019
56. Sagna P, Ndiaye O, Diop C, Niang AD, Sambou PC. Les variations recentes du climat constatees au Senegal sont-elles en phase avec les descriptions donnees par les scenarios du GIEC? *Pollut Atmos.* 2015;227:1-17.
doi: 10.4267/pollution-atmospherique.5320
57. Ringard J. *Etude Rétrospective et Prospective des Vagues de Chaleur en Afrique de l'Ouest. University Jos Four, Gre*. Available from: https://www.researchgate.net/profile/justine-ringard/publication/260018793_etude_retrospective_et_prospective_des_vagues_de_chaleur_en_afrique_de_l%27ouest/links/02e7e52f12bf345bcd000000/etude-retrospective-et-prospective-des-vagues-de-chaleur-en-afrique-de-louest.pdf [Last accessed on 2025 Mar 08].
58. Stone DA, Weaver AJ. Daily maximum and minimum temperature trends in a climate model. *Geoph Res Lett.* 2002;29(9):70-1-70-4.
doi: 10.1029/2001GL014556
59. Braganza K, Karoly DJ, Arblaster JM. Diurnal temperature range as an index of global climate change during the twentieth century. *Geophys Res Lett.* 2004;31(13):1-4.
doi: 10.1029/2004GL019998
60. Easterling DR, Meehl GA, Parmesan C, Changnon SA, Karl TR, Mearns LO. Climate extremes: Observations, modeling, and impacts. *Science.* 2000;289(5487):2068-2074.
doi: 10.1126/science.289.5487.2068
61. Hartmann DL, Tank AMK, Rusticucci M, *et al*. *Observations: Atmosphere and Surface.* Cambridge United Kingdom and NY, USA: Cambridge University Press; 2013. p. 195-254. Available from: https://www.ipcc.ch/site/assets/uploads/2017/09/wg1ar5_chapter02_final.pdf [Last accessed on 2025 Mar 08].
62. Trigo RM, García-Herrera R, Díaz J, Trigo IF, Valente MA. How exceptional was the early August 2003 heatwave in France? *Geophys Res Lett.* 2005;32(10):L10701.
doi: 10.1029/2005GL022410open_in_new
63. Rome S, Caniaux G, Ringard J, Dieppois B, Diedhiou A. Identification de Tendances Recentes et Ruptures D'homogeneite des Temperatures: Exemple en Afrique de l'Ouest et sur le Golfe de Guinee. In: *28ème Colloquim Internationale de l'AIC, Liège, Belgium*; 2015. p. 591-596.
64. Barbier J. *Extrêmes Climatiques: Les Vagues de Chaleur au Printemps Sahelien*. Universoty de Toul. Available from: https://theses.hal.science/tel-04225047v1/document [Last accessed on 2025 Mar 12].
65. Meehl GA, Tebaldi C. More intense, more frequent, and longer lasting heat waves in the 21st Century. *Science.* 2004;305(5686):994-997.
doi: 10.1126/science.1098704